THE JOURNAL OF BIOLOGICAL CHEMISTRY VOL. 290, NO. 51, pp. 30551–30561, December 18, 2015
Published in the U.S.A.

Coupling between Nutrient Availability and Thyroid Hormone Activation*

Received for publication, May 14, 2015, and in revised form, October 13, 2015 Published, JBC Papers in Press, October 23, 2015, DOI 10.1074/jbc.M115.665505

Lattoya J. Lartey[‡], João Pedro Werneck-de-Castro[§¶], InSug O-Sullivan[‖], Terry G. Unterman[‖], and Antonio C. Bianco[§1]

From the [‡]Department of Molecular and Cellular Pharmacology, University of Miami, Miller School of Medicine, Miami, Florida 33136, the [§]Department of Internal Medicine, Division of Endocrinology and Metabolism, Rush University Medical Center, Chicago, Illinois 60612, the [¶]Carlos Chagas Filho Biophysics Institute and School of Physical Education and Sports, Federal University of Rio de Janeiro, Rio de Janeiro 21941-599, Brazil, and the [‖]Jesse Brown Veterans Affairs Medical Center and the Department of Medicine, University of Illinois at Chicago College of Medicine, Chicago, Illinois 60612

Background: Insulin/IGF-1 stimulates thyroid hormone action via type 2 deiodinase (D2).
Results: Insulin/IGF-1-induced activation of the PI3K-mTORC2-Akt pathway transcriptionally up-regulates D2.
Conclusion: FOXO1 represses *DIO2* during fasting, and derepression occurs via nutritional activation of the PI3K-mTORC2-Akt pathway.
Significance: This mechanism explains how T_3 production, serum T_3 levels, and T_3-dependent cellular metabolic rate are kept at a level proportionate to the availability of energy substrates.

The activity of the thyroid gland is stimulated by food availability via leptin-induced thyrotropin-releasing hormone/thyroid-stimulating hormone expression. Here we show that food availability also stimulates thyroid hormone activation by accelerating the conversion of thyroxine to triiodothyronine via type 2 deiodinase in mouse skeletal muscle and in a cell model transitioning from 0.1 to 10% FBS. The underlying mechanism is transcriptional derepression of *DIO2* through the mTORC2 pathway as defined in rictor knockdown cells. In cells kept in 0.1% FBS, there is *DIO2* inhibition via FOXO1 binding to the *DIO2* promoter. Repression of *DIO2* by FOXO1 was confirmed using its specific inhibitor AS1842856 or adenoviral infection of constitutively active FOXO1. ChIP studies indicate that 4 h after 10% FBS-containing medium, FOXO1 binding markedly decreases, and the *DIO2* promoter is activated. Studies in the insulin receptor FOXO1 KO mouse indicate that insulin is a key signaling molecule in this process. We conclude that FOXO1 represses *DIO2* during fasting and that derepression occurs via nutritional activation of the PI3K-mTORC2-Akt pathway.

In mammals, body energy expenditure is gradually decreased with caloric restriction as well as prolonged starvation. This is an adaptive response driven by the hypothalamus that includes behavioral as well as metabolic modifications, such as increased sleep, diminished motor activity, and core temperature (1). During fasting, the hormonal milieu is dominated by low levels of insulin and thyroid hormones, which has been proposed as an explanation for the slowdown in weight loss after a few days of caloric restriction (2, 3). Notably, thyroidal activity is restored promptly upon refeeding, as seen in patients recovering from anorexia nervosa (4). In such patients, weight gain and an increase in serum T_3[2] are closely associated with acceleration in energy expenditure (4). These observations indicate that the set point at which the hypothalamic-pituitary-thyroid activity is maintained is affected by nutrient availability, with the lowest (default) levels of activity seen during caloric restriction. Leptin is the key molecule signaling food intake and the availability of energy substrates, which defines the hypothalamic-pituitary-thyroid set point by stimulating secretion of thyrotropin-releasing hormone and thyroid-stimulating hormone and hence thyroidal activity (5, 6).

In humans, the thyroid gland contributes with about 20% of the daily T_3 production, and the residual 80% is contributed by two deiodinases that convert T_4 to T_3 outside the thyroid parenchyma (*i.e.* D1 and D2, with the latter playing the major role) (7). *In vivo* kinetic studies in rats indicate that serum T_3 levels fall during fasting also as a result of decreased thyroidal T_3 secretion (8). In addition, there is also accelerated thyroid hormone inactivation via D3 expression in multiple tissues as well as accelerated sulfation and glucuronidation in the liver (9, 10). However, it is less clear whether the extrathyroidal T_3 production is reduced as well. Whereas hepatic D1 activity is reduced during caloric restriction in rodents (11), this seems to be a consequence rather than a cause of the low serum T_3, given that *Dio1* is highly responsive to T_3 (8, 12). On the other hand, D2 is normally stimulated during hypothyroidism (7), and the fact that it is reduced by fasting in the pituitary gland and brown

* This work was supported in part by National Institutes of Health, NIDDK, Grant DK65055 and by a grant from the Department of Veterans Affairs Merit Review Program (to T. G. U.). The authors declare that they have no conflicts of interest with the contents of this article. The content is solely the responsibility of the authors and does not necessarily represent the official views of the National Institutes of Health.

[1] To whom correspondence should be addressed: Dept. of Internal Medicine, Division of Endocrinology and Metabolism, Rush University Medical Center, 1735 W. Harrison St., Cohn Bldg. Rm. 212, Chicago, IL 60612. Tel.: 312-942-7131; Fax: 312-942-5271; E-mail: abianco@deiodinase.org.

[2] The abbreviations used are: T_3, triiodothyronine; T_4, thyroxine; TR, T_3 receptor; D1, D2, and D3, type 1, 2, and 3 deiodinase, respectively; CA, constitutively active; BAT, brown adipose tissue; mTOR, mammalian target of rapamycin; MTORC1 and -2, mTOR complex 1 and 2, respectively; qPCR, quantitative PCR; BisTris, 2-[bis(2-hydroxyethyl)amino]-2-(hydroxymethyl)propane-1,3-diol; NSC, non-silencing control; IR, insulin receptor; LIRKO, liver-specific IR knock-out; LIRFKO, IR/FOXO1 double knock-out; IGF, insulin-like growth factor.

adipose tissue (BAT) (10) indicates a role in the fall of serum T_3. D2 is an endoplasmic reticulum-resident protein that increases intracellular T_3 concentration and the expression of thyroid hormone-dependent genes (7, 13). For example, approximately half of the T_3 present in the brain and in the BAT is originated locally via D2 activity; D2 inactivation in both tissues has been shown to dampen thyroid hormone signaling (7). Therefore, control of the D2 pathway by caloric intake could potentially modulate thyroid hormone signaling by affecting intracellular T_3 concentration as well as circulating T_3 levels.

D2 expression is controlled by transcriptional (*i.e.* cAMP, FOXO3, and NF-κB) (14, 15), translational (*i.e.* ER stress) (16), and post-translational mechanisms, such as ubiquitination and proteasomal degradation (17). In addition, D2 activity in rat BAT is up-regulated by growth factors such as IGF-1 and the multifunctional protein insulin (18, 19), which promotes cellular glucose uptake and growth by acting through various nutrient-sensing pathways, such as the PI3K-mTOR signaling pathway. Mammalian target of rapamycin (mTOR) is a signaling pathway that functions as a regulator of translational initiation for cellular metabolism, growth, survival, proliferation, and protein synthesis (20, 21). mTOR, a 289-kDa Ser/Thr kinase, serves as the catalytic core of two distinct multicomponent complexes, mTOR complex 1 (mTORC1) and mTOR complex 2 (mTORC2) (22). Numerous studies have linked mTORC1 to protein synthesis and growth (23) and to the downstream activation of a myriad of metabolic regulatory genes, including *HIF-1α* and *SREBP1/2* (24). In addition, it has been determined that mTORC2 phosphorylates the AGC kinases (25) and mediates cell survival and proliferation through phosphorylation of its downstream effector, Akt (26).

The observation that insulin stimulates D2 activity in rat brown adipocytes (19) and that insulin sensitizers stimulate D2 expression in cultures of skeletal myocytes (27) indicate that the nutritional state of an organism can also affect thyroid hormone signaling by acting at the target cell level. The mechanism behind D2 stimulation by insulin remain unknown, despite evidence that an indirect effect via the adrenergic receptors could play a role (28). In the present study, we have examined how nutrient availability and insulin stimulate D2 activity in mice and cell models. We have found that insulin signals through PI3K-mTORC2-Akt to relieve FOXO1-mediated repression of *DIO2*, indicating that nutrient availability controls serum levels of thyroid hormones not only by modulating the hypothalamic-pituitary-thyroid set point but also by regulating extrathyroidal T_3 production. Given that serum T_3 is a major determinant of energy expenditure (29), this explains how the cellular metabolic rate as defined by T_3 signaling is kept at a level that is commensurate to the availability of energy substrates.

Experimental Procedures

Reagents and Antibodies—Outer ring-labeled [^{125}I]T_4 (specific activity 4400 Ci/mmol; PerkinElmer Life Sciences) was purified on LH-20 columns before use; fetal bovine serum (FBS) was from Atlanta Biologicals (Flowery Branch, GA); cycloheximide, insulin, IGF-1, LY294002, wortmannin, GSK609693, rapamycin, and PP242 were from Sigma-Aldrich; AS1842856 was from EMD Millipore (Billerica, MA); α-phospho-S6rp (Ser-235/236), α-phospho-S6rp (Ser-240/244), α-total S6rp, α-phospho-Akt (Ser-473), α-phospho-Akt (Thr-308), α-pan-Akt, α-phospho-4EBP1, α-total 4EBP, α-total rictor, α-total raptor, α-phospho-FOXO1 (Ser-256), and α-total FOXO1 were from Cell Signaling Technology (Boston, MA); GAPDH antibody was from GeneTex (Irvine, CA); α-FKHR (H-128) was from Santa Cruz Biotechnology, Inc. (Dallas, TX).

Cell Culture—MSTO-211H cells were from American Type Culture Collection (Manassas, VA) and cultured in humidified atmosphere with 5% CO_2 at 37 °C, in RPMI 1640 from CellGro (Manassas, VA) supplemented with 10% FBS and 100 nM sodium selenite (16, 30). As indicated, cells were serum-starved for 48 h in 0.1% FBS medium prior to re-exposure to 10% FBS medium, insulin stimulation, or IGF-1 stimulation.

Deiodinase Assays—After harvesting, tissues and MSTO-211H cells were resuspended in Dulbecco's PBS containing 1 mM EDTA (PE), 0.25 M sucrose, and 10 mM dithiothreitol (DTT) and sonicated, and cell lysates were analyzed for protein concentration via Bradford assay (Bio-Rad). D2 assays were performed as described previously in duplicate (27).

Gene Expression Analysis—RNA was extracted from MSTO-211H cells or animal tissue using the RNAqueous Micro Kit (Life Technologies Inc.) or RNeasy Mini Kit (Qiagen), respectively. RNA was quantified with a NanoDrop and reverse transcribed using High Capacity cDNA (Applied Biosystems) or the First Strand cDNA for RT-PCR (AMV) Kit (Roche Applied Science). Genes of interest were measured by qPCR (Bio-Rad *iCycler* iQ real-time PCR detection system) using the iQ SYBR Green Supermix (Bio-Rad) or qPCR (Applied Biosystems Step One Plus Real-Time PCR System) using the SYBR Green FastMix ROX (Quanta Biosciences). Relative quantitation was using the standard curve method and the iCycler or Step One Plus software.

Western Blot Analysis—Cells/tissues were lysed in 0.25 M sucrose PE containing 10 mM DTT. The lysates were diluted with 4× sample loading buffer (Invitrogen), and 5–25 μg of total protein were run on 4–12% NuPAGE BisTris gels (Life Technologies, Inc.). Samples were transferred to Immobilon-FL PVDF transfer membrane (Millipore, Billerica, MA) and probed with antibodies as indicated at a 1:1000 dilution overnight. Fluorescent labeled secondary antibodies (LI-COR Biosciences, Lincoln, NE) were used at 1:2500 for 1 h. All blots were imaged using the LI-COR Odyssey instrument per the manufacturer's instructions.

T_4 to T_3 Conversion in Intact Cells—The production of T_3 from outer ring-labeled T_4 in intact cells was analyzed by measuring ^{125}I in the medium as described elsewhere (31) except that the assay was stopped 12 h after the addition of [^{125}I]T_4, and the free T_4 concentration was 30 pM.

Lentivirus-mediated shRNA Knockdown of Rictor and Raptor—Rictor and raptor knockdown were established by transduction with GIPZ lentiviral shRNAmir vectors in MSTO-211H cells using GIPZ lentiviral shRNAmir for non-silencing control (NSC), human rictor (clone ID V2LHS_120392 and clone ID V3LHS_367492), or human raptor (clone ID V3LHS_636800) from Thermo Scientific (Lafayette, CO). For generation of stable knockdown cell lines, MSTO-211H cells were plated at 1.5×10^5 cells/well and transduced with

lentiviral particles at a multiplicity of infection of ~23 and ~15 for rictor, respectively, and a multiplicity of infection of ~13 for raptor and diluted in 1 ml of serum-free RPMI containing 8 μg/ml Polybrene (Sigma-Aldrich). After 6 h, 1 ml of complete RPMI was added to each well (6-well plates). 72 h later, the transfection mixture was replaced with complete medium containing puromycin (1 μg/ml) to select for shRNA-expressing cells. Stable cell lines were generated after puromycin selection for 7 days.

Adenovirus-mediated Transduction of WT and Constitutively Active (CA) FOXO1—Adenoviral particles expressing WT and CA FOXO1 as described (32) were used to generate transient transfections for WT and CA FOXO1 in MSTO-211H. Cells were plated at 2.5×10^5 cells/well in 6-well dishes and transduced with adenoviral particles of concentration 2.0×10^{10} pfu/ml and 1.8×10^{10} pfu/ml, respectively, that were diluted in 1 ml of serum-free RPMI. Complete medium containing 10% FBS was added after 6 h, and the medium was changed again after 24 h. At 48 h, cells were refed or stimulated with insulin for the experimental procedure.

Animal Studies—All studies performed were approved by the institutional animal care and use committee of the University of Miami in compliance with National Institutes of Health Standards. Male, 3-month-old C57BL/6J mice purchased from Jackson Laboratory were housed at room temperature (22 °C) on a 12-h dark/light cycle. Mice were randomly divided into three groups (control, fasting, refeeding) and acclimatized for 5 days. Animals were fed *ad libitum* with a standard chow diet (3.5 kcal/g, 28.8% protein, 58.5% carbohydrate, 12.7% fat; 5010 LabDiet laboratory autoclavable rodent diet; PMI Nutrition, Richmond, IN) and water. When indicated, food was withdrawn at 21:00 h for the fasting and refeeding groups. After 36 h, fasted mice were sacrificed by asphyxiation in a CO_2 chamber. Mice from the refeeding group were weighed, refed for 8 h, and sacrificed. Soleus muscle and cortex were rapidly dissected and frozen in liquid nitrogen and stored at −80 °C until analysis. As indicated, freely feeding 11-week-old male insulin receptor (IR) floxed, liver-specific IR knock-out (LIRKO), and IR/FOXO1 double knock-out (LIRFKO) mice (33) were used as well. They were sacrificed by decapitation following brief sedation with isofluorane.

Blood Biochemistry—Blood was collected by cardiac puncture, and plasma was stored at −80 °C until analysis. Insulin was measured using mouse insulin ELISA (Mercodia, AB). Serum T_3 and T_4 were measured as described previously (34).

Chromatin Immunoprecipitation—ChIP was performed using the EZ-ChIP chromatin immunoprecipitation kit (EMD Millipore) according to the manufacturer's guidelines. Primers for RT-qPCR (Applied Biosystems Step One Plus Real-Time PCR System) were designed for predicted FOXO1 binding sites in the *DIO2* promoter region (forward, 5′-CTGTCTGGAGGAACTTGGATTT-3′; reverse, 5′-CCATGACTCCAACCCTTTGT-3′), and qPCR was performed using the SYBR Green FastMix ROX (Quanta Biosciences).

Statistical Analysis—All data were analyzed using PRISM software (GraphPad Software) and expressed as mean ± S.E. Student's *t* test was used to compare two groups. One-way analysis of variance was used to compare more than two groups. Significance was held at $p < 0.05$ (two-tailed).

Results

Fasting Lowers Soleus Dio2 mRNA Expression Levels and Activity in Mice—Fasting for 36 h caused a marked loss in body weight (Fig. 1*A*), a drop in serum insulin levels (Fig. 1*B*), and insulin signaling in skeletal muscle (Fig. 1*C*). This was associated with an ~80% reduction in soleus *Dio2* mRNA levels (Fig. 1*D*) and D2 activity (Fig. 1*E*). The decrease in D2 expression and activity was tissue-specific given that cerebral cortex *Dio2* mRNA remained stable throughout the fasting period (Fig. 1*F*). This led to a ~45% reduction in serum T_3 levels (0.56 ± 0.11 *versus* 0.29 ± 0.06 ng/ml; $n = 4$; $p < 0.01$), whereas serum T_4 remained largely unaffected (59 ± 12 *versus* 53 ± 10 ng/ml; $n = 4$; not significant). Refeeding for 8 h normalized body weight (Fig. 1*A*), increased serum insulin levels by about 100-fold (Fig. 1*B*), increased insulin signaling (Fig. 1*C*), elevated *Dio2* mRNA (Fig. 1, *G* and *H*) and activity levels (Fig. 1*I*), normalized serum T_3 (0.48 ± 0.09 ng/ml; $n = 4$), and did not affect serum T_4 (54 ± 13 ng/ml; $n = 4$).

Fresh Serum Induces D2 Expression in a Cell Model—Given that D2 activity is near background level in skeletal muscle cell lines (27), the role played by fasting and refeeding on *DIO2* expression was next modeled using MSTO-211H cells, a cell line that endogenously expresses readily measurable D2 activity (30). In this setting, keeping the cells for 48 h in 0.1% FBS caused a progressive reduction in *DIO2* mRNA and activity to approximately half of the baseline values seen in cells cultured in 10% FBS (Fig. 2outf;F2, *A* and *B*). Notably, transition to 10% FBS resulted in a ~3.5-fold increase in D2 activity (Fig. 2*C*) that followed a ~2-fold increase in D2 mRNA levels (Fig. 2*D*); both subsided and returned to baseline levels by 24 h (Fig. 2, *C* and *D*). The increases in D2 activity (Fig. 2*E*) and typical serum-dependent downstream targets (Fig. 2*F*) were dependent on the amount of FBS contained in the fresh medium. D2 is known for having a post-translational regulation via ubiquitination and proteasomal degradation, explaining its relatively short activity half-life of less than 1 h (35). Thus, we tested whether the surge in D2 activity that follows refeeding could also involve the ubiquitin-proteasomal mechanism. D2 activity half-life was measured by exposing cells in 10% FBS to cyclohexamide, but at no time was there a significant effect on D2 activity half-life (Fig. 2, *G–J*).

PI3K-dependent Pathways Stimulate D2 Activity—Serum/FBS contains a number of growth factors that could potentially induce D2 expression during refeeding, mostly acting via PI3K. Thus, we used insulin and observed a concentration-dependent increase in D2 activity of ~50% after 8 h (Fig. 2*K*). We also observed a time-dependent increase in D2 activity following the stimulation of serum-starved MSTO-211H cells with 50 ng/ml IGF-1 (Fig. 2*L*). The acceleration in D2 activity increased thyroid hormone activation, given that T_3 production was accelerated 4–5-fold after the addition of IGF-1 or insulin (Fig. 2*M*). Next, different strategies were used to dissect the molecular pathway that mediates the insulin/IGF-1 stimulation of *DIO2* expression. First, we inhibited PI3K using LY294002, a well known reversible inhibitor of PI3K phosphorylation. Following

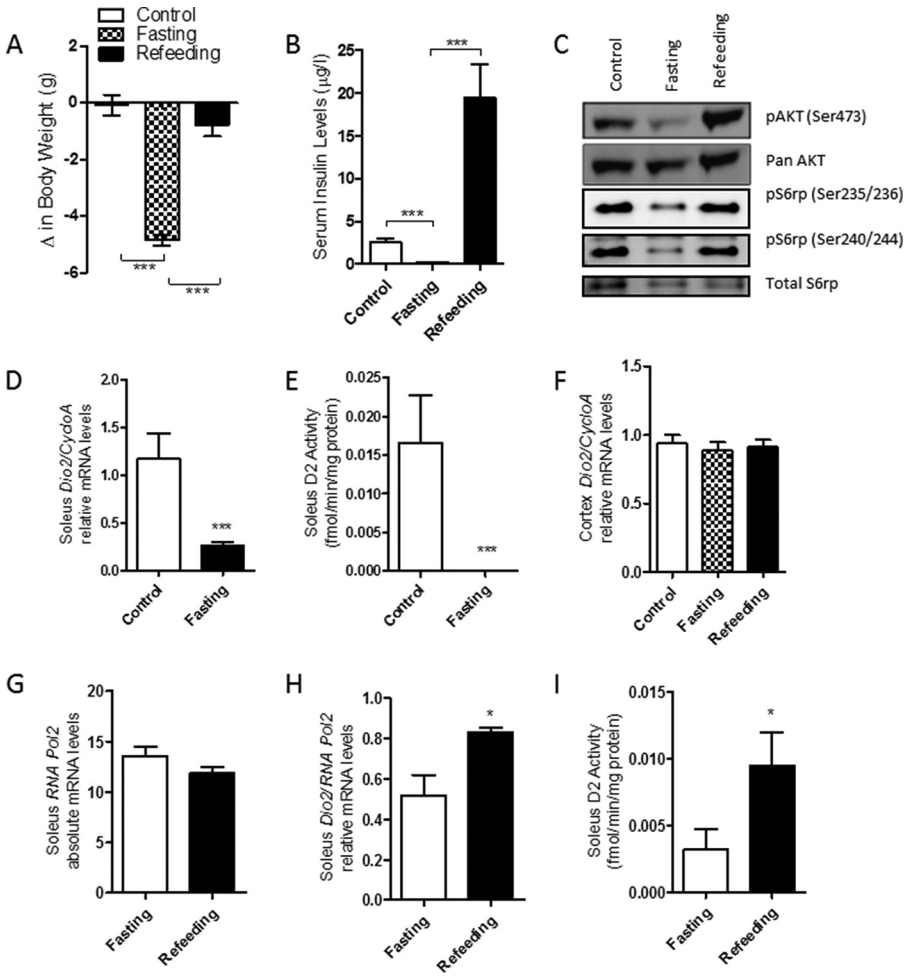

FIGURE 1. **Fasting inhibits Dio2 expression levels and activity in the soleus muscle of mice.** *A*, change in body weight of control, fasted, and refed mice measured before and after the experimental period; $n = 7$; ***, $p < 0.001$. *B*, serum insulin levels measured in control, fasted, and refed mice; $n = 10, 12, 7$, respectively; ***, $p < 0.001$. *C*, Western blot analysis of control, fasting, and refeeding groups using α-total S6rp, α-phospho-S6rp (Ser-235/236/240/244), α-pan-Akt, and α-phospho-Akt (Ser-473) antibodies. *D*, *CycloA* was used as a housekeeping gene for the measurement of relative mRNA levels of *Dio2/CycloA* in the soleus muscle; $n = 3$ (control), $n = 6$ (fasting); ***, $p < 0.001$. *E*, D2 activity measured in soleus muscle of control and fasted mice; $n = 3$ and 7, respectively; ***, $p < 0.001$. *F*, *CycloA* was used as a housekeeping gene for the measurement of relative mRNA levels of *Dio2/CycloA* in the cortex; $n = 7$. *G*, RNA polymerase 2 was used as a housekeeping gene; $n = 7$. *H*, the measurement of relative mRNA levels of *Dio2/RNAPol2* in soleus muscle; $n = 7$; *, $p < 0.05$. *I*, D2 activity measured in the soleus muscle of fasted and refed mice; $n = 7$; *, $p < 0.05$. *Error bars*, S.E.

the standard 48 h starvation period in 0.1% FBS, MSTO-211H cells were treated with 50 μM LY294002 and either stimulated with 10% FBS (Fig. 3*A*) or exposed to insulin (Fig. 3*B*). Notably, inhibition of PI3K abrogated the increase in D2 activity at all time points studied, which coincided with the inhibition of phosphorylation of the downstream targets Akt and S6rp (Fig. 3, *A* and *B*). Similar results were observed when 0.1–1 μM wortmannin was used to inhibit PI3K signaling (Fig. 3*C*, *a* and *b*). Next, we looked further down the pathway and used GSK690693, an inhibitor of all three Akt isoforms (36, 37) to examine the involvement of Akt in this mechanism. MSTO-211H cells that had been starved for 48 h were pretreated for 1 h with 10 nM GSK690693 (37) and subsequently exposed to insulin. Again, insulin induction of D2 activity was prevented at all time points tested throughout a 24 h time period (Fig. 3*D*). Western blot analysis of Akt phosphorylation shows overstimulation of the Akt pathway, a feature commonly observed when small molecule Akt inhibitors are used (36, 37). This was coupled with inhibition of S6rp phosphorylation (Fig. 3*D*), indicating successful Akt inhibition.

Inhibition of mTOR Pathway Prevents FBS and Insulin-mediated D2 Stimulation—We next used PP242, a selective ATP-competitive inhibitor of both mTORC1 and mTORC2 (38, 39) to test the involvement of the mTOR signaling pathway in the D2 stimulation by FBS or insulin. Treating cells with 2 μM PP242 prevented the surge in D2 activity that follows 10% FBS (Fig. 4*A*) or insulin stimulation (Fig. 4*B*). The effectiveness of PP242 in blocking both the mTORC1 and mTORC2 signaling pathways was documented by Western blot analysis of downstream targets of mTORC1 (S6rp and 4EBP1) and of mTORC2 (Akt) (Fig. 4, *A* and *B*). Next, we used rapamycin, an inhibitor of mTORC1 (40), to further investigate the involvement of the mTOR pathway. Inhibition of mTORC1 delayed but did not prevent the surge in D2 activity caused by 10% FBS (Fig. 4*C*). Inhibitory selectivity was documented by Western blot analysis of phosphorylated and total S6rp, a downstream marker of mTORC1. Indeed, there was reduction of mTORC1 signaling after 4 h of rapamycin treatment, whereas phosphorylation of Akt via mTORC2 was not inhibited (Fig. 4*D*). Similar to D2 activity, we also found a significant increase of *DIO2* mRNA

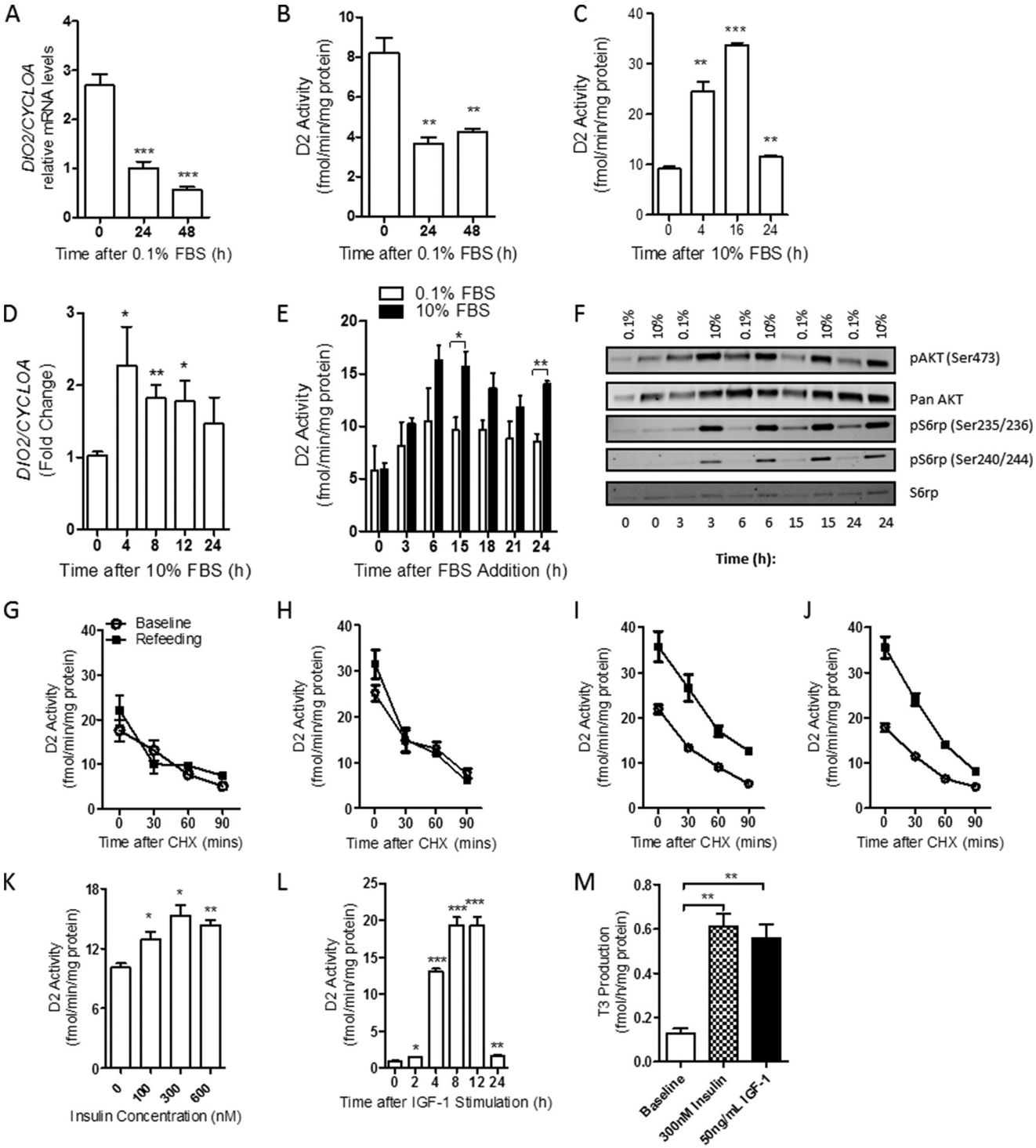

FIGURE 2. **Nutrient availability increases D2 activity via transcriptional activation of DIO2 in MSTO-211H cells.** *A* and *B*, *DIO2* mRNA expression levels (*A*) and D2 activity (*B*) measured during 48 h of starvation in 0.1% FBS; $n = 3$; ***, $p < 0.001$ *versus* 0 h; **, $p < 0.01$ *versus* 0 h. *C*, D2 activity following the addition of 10% FBS; $n = 3$; **, $p < 0.01$ *versus* 0 h; ***, $p < 0.001$ *versus* 0 h. *D*, *DIO2* expression levels measured by -fold change of *DIO2/CYCLOA* following the addition of 10% FBS; $n = 3$; *, $p < 0.05$ *versus* 0 h; **, $p < 0.01$ *versus* 0 h. *E*, D2 activity following 48 h of serum starvation in 0.1% FBS prior to the addition of 0.1 or 10% FBS supplemented medium. Cells were harvested at the indicated time points; $n = 3$; *, $p < 0.05$; **, $p < 0.01$. *F*, Western blot analysis at the indicated time points using α-total S6rp, α-phospho-S6rp (Ser-235/236/240/244), α-pan-Akt, and α-phospho-Akt (Ser-473) antibodies. *G–J*, assessment of D2 half-life using cyclohexamide (*CHX*) as a translational inhibitor 4 h (*G*), 0 h (*H*), 8 h (*I*), and 12 h (*J*) following the addition of 10% FBS. Cells were harvested at the indicated time points; $n = 3$. *K*, D2 activity following 8 h of insulin stimulation with 0, 100, 300, or 600 nM insulin supplemented with 0.1% FBS; $n = 3$; *, $p < 0.05$ *versus* 0 nM; **, $p < 0.01$ *versus* 0 nM. *L*, D2 activity measured following 48 h of serum starvation prior to stimulation with 50 ng/ml IGF-1; $n = 3$; *, $p < 0.05$; **, $p < 0.01$; ***, $p < 0.001$. *M*, T_3 production measured in intact MSTO-211H cells 12 h after 300 nM insulin or 50 ng/ml IGF-1 stimulation. T_3 production was calculated based on the free ^{125}I content in the medium; $n = 3$; **, $p < 0.01$. *Error bars*, S.E.

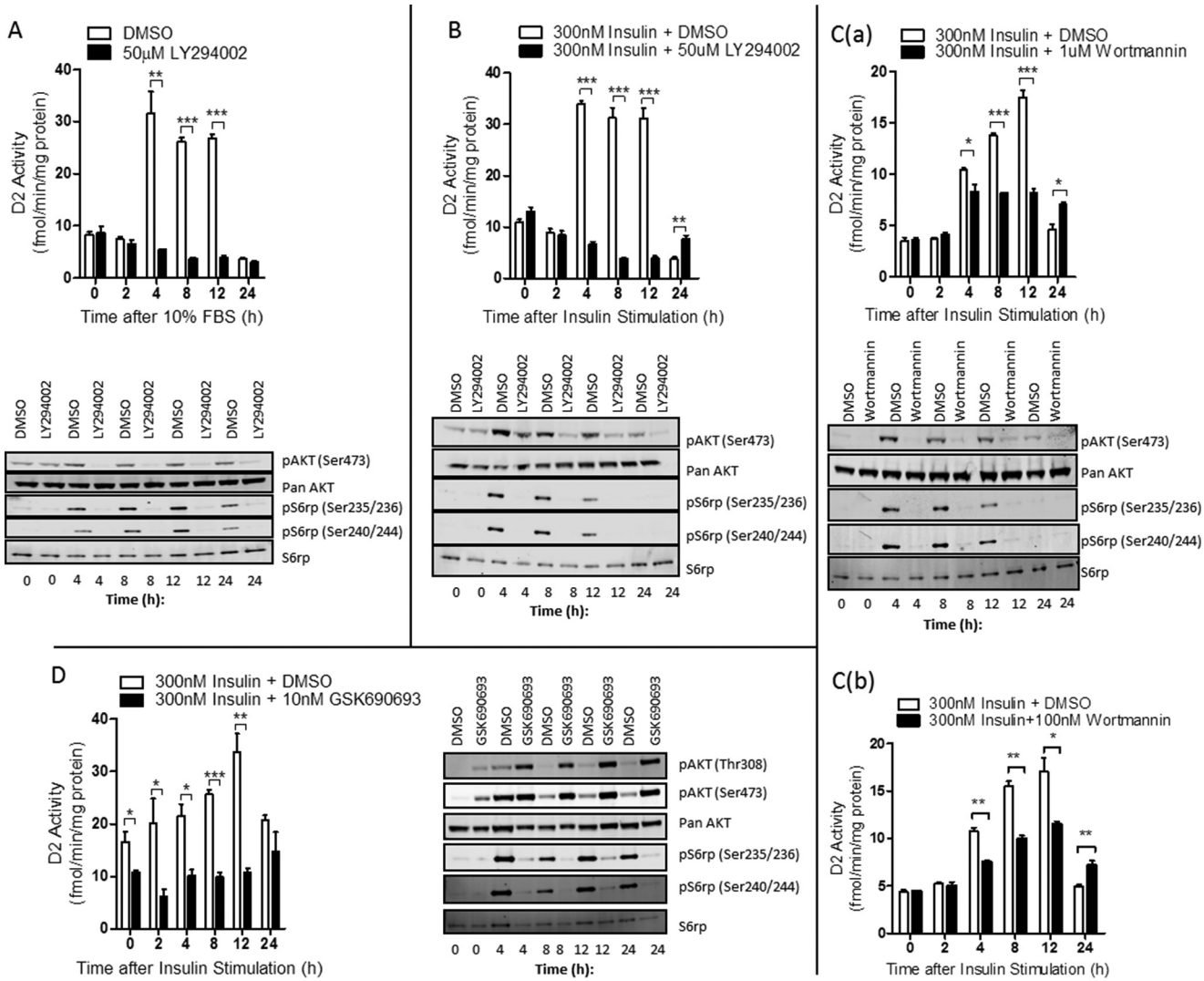

FIGURE 3. **Inhibition of PI3K signaling using LY294002 and wortmannin or of Akt signaling using GSK690693 prevents the insulin-induced increase in D2 activity in MSTO-211H cells.** *A*, *top*, D2 activity following 48 h of starvation in 0.1% FBS prior to the addition of 10% FBS along with 50 μM LY294002; $n = 3$; **, $p < 0.01$; ***, $p < 0.001$. *Bottom*, corresponding Western blot analysis at the indicated time points using α-total S6rp, α-phospho-S6rp (Ser-235/236/240/244), α-pan-Akt, and α-phospho-Akt (Ser-473) antibodies. *B*, *top*, D2 activity following 48 h of starvation in 0.1% FBS prior to 300 nM insulin stimulation along with 50 μM LY294002; $n = 3$; ***, $p < 0.001$; **, $p < 0.01$. *Bottom*, corresponding Western blot analysis at the indicated time points using α-total S6rp, α-phospho-S6rp (Ser-235/236/240/244), α-pan-Akt, and α-phospho-Akt (Ser-473) antibodies. *C*(*a*), D2 activity following 48 h of starvation in 0.1% FBS prior to 300 nM insulin stimulation along with 1 μM wortmannin; $n = 3$; *, $p < 0.05$; ***, $p < 0.001$; corresponding Western blot analysis at the indicated time points using α-total S6rp, α-phospho-S6rp (Ser-235/236/240/244), α-pan-Akt, and α-phospho-Akt (Ser-473) antibodies. *C*(*b*), D2 activity following 48 h of starvation in 0.1% FBS and 3 h of preinhibition with 100 nM wortmannin prior to the addition and 300 nM insulin stimulation; $n = 3$; *, $p < 0.05$; **, $p < 0.01$. *D*, *left*, D2 activity following 48 h of starvation in 0.1% FBS and 3 h of 100 nM preinhibition with wortmannin prior to the addition of 10 nM GSK690693 and 300 nM insulin stimulation; $n = 3$; *, $p < 0.05$; **, $p < 0.01$; ***, $p < 0.001$. *Right*, corresponding Western blot analysis at the indicated time points using α-total S6rp, α-phospho-S6rp (Ser-235/236/240/244), α-pan-Akt, and α-phospho-Akt (Ser-473 and Thr-308) antibodies. *Error bars*, S.E.

levels at various time points over a 24 h period (Fig. 4*E*). Studies with insulin led to similar observations (Fig. 4*F*). As further confirmation, we used GIPZ lentiviral shRNA vectors to knockdown raptor (regulatory-associated protein of mTOR), a component of the mTORC1 complex. Despite successful raptor knockdown in these cells, both 10% FBS (Fig. 5*A*) and the addition of insulin (Fig. 5*B*) stimulated D2 activity. Altogether, these data suggest that D2 induction by 10% FBS or exposure to insulin is mediated by an mTORC2-dependent pathway.

To assess the role played by mTORC2, we next used GIPZ lentiviral shRNA vectors to knock down an essential component of the mTORC2 complex, rictor (rapamycin-insensitive component of mTOR) in MSTO-211H cells. Rictor is a core unit of the mTORC2 complex, and its reduction disrupts mTORC2 complex assembly (41). Stably expressing cells were starved for 48 h prior to the addition of 10% FBS (Fig. 5*C*) or insulin stimulation (Fig. 5*D*). Inhibition of mTORC2 significantly inhibits the surge in D2 activity at all time points tested, peaking at a 4-fold reduction by 12 h in both conditions as compared with NSCs. The successful knockdown of rictor was documented by Western blot. These data show the dependence of induction of D2 activity on the mTORC2 pathway.

FOXO1 Transcriptionally Represses DIO2—While looking for the mTORC2/Akt-dependent downstream targets that could activate *DIO2*, we serendipitously observed that *Dio2* mRNA levels were low in a mouse with liver-specific inactiva-

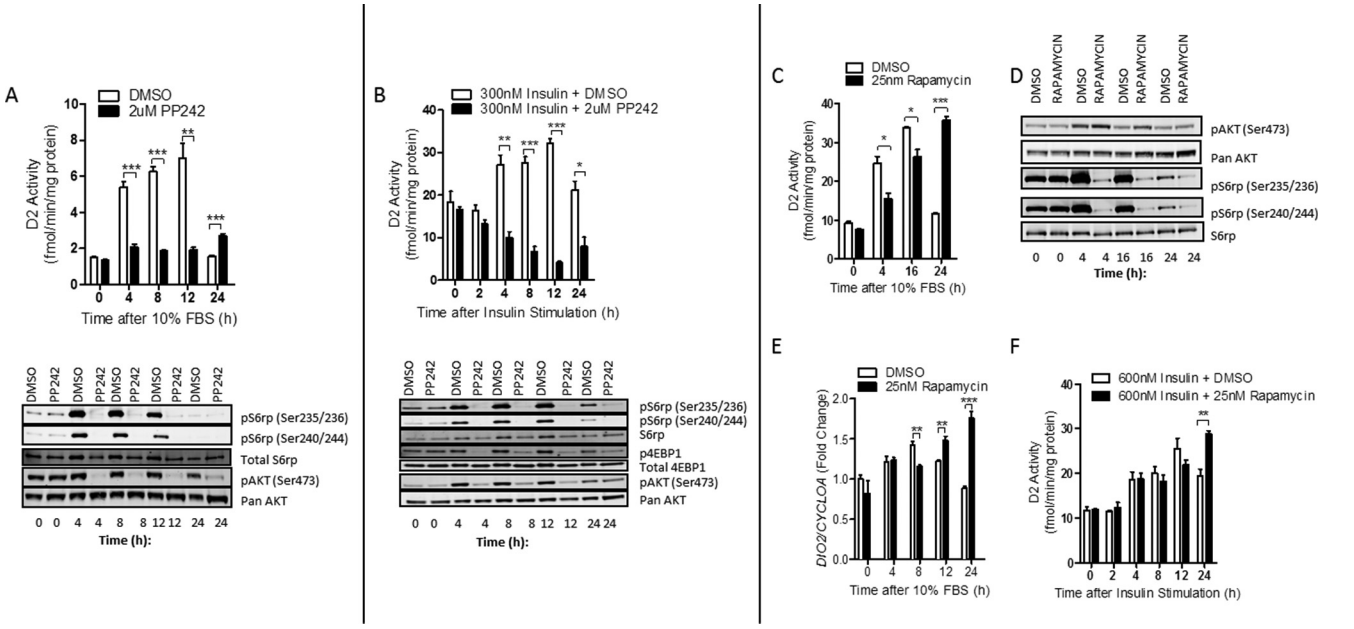

FIGURE 4. **Inhibition of mTOR signaling using PP242 prevents FBS- and insulin-mediated D2 stimulation; however, inhibition of mTORC1 signaling using rapamycin has no effect on the insulin-induced increase in D2 activity in MSTO-211H cells.** *A*, *top*, D2 activity following 48 h of starvation in 0.1% FBS prior to the addition of 10% FBS along with 2 μM PP242; $n = 3$; **, $p < 0.01$; ***, $p < 0.001$. *Bottom*, corresponding Western blot analysis at the indicated time points using α-total S6rp, α-phospho-S6rp (Ser-235/236/240/244), and α-pan-Akt and α-phospho-Akt (Ser-473) antibodies. *B*, *top*, D2 activity following 48 h of starvation in 0.1% FBS prior to 300 nM insulin stimulation along with 2 μM PP242; $n = 3$; **, $p < 0.01$; ***, $p < 0.001$; *, $p < 0.05$. *Bottom*, corresponding Western blot analysis at the indicated time points using α-total S6rp, α-phospho-S6rp (Ser-235/236/240/244), α-total 4EBP1, α-phospho-4EBP1, α-pan-Akt, and α-phospho-Akt (Ser-473) antibodies. *C*, D2 activity following 48 h of starvation in 0.1% FBS prior to the addition of 10% FBS along with 25 nM rapamycin; $n = 3$; *, $p < 0.05$; ***, $p < 0.001$. *D*, Western blot analysis at the indicated time points using α-total S6rp, α-phospho-S6rp (Ser-235/236/240/244), α-pan-Akt, and α-phospho-Akt (Ser-473) antibodies. *E*, *DIO2* expression levels measured as -fold change of *DIO2/CYCLOA* at the indicated time points; $n = 3$; **, $p < 0.01$; ***, $p < 0.001$. *F*, D2 activity following 48 h of starvation in 0.1% FBS prior to 600 nM insulin stimulation along with 25 nM rapamycin; $n = 3$; **, $p < 0.01$. *Error bars*, S.E.

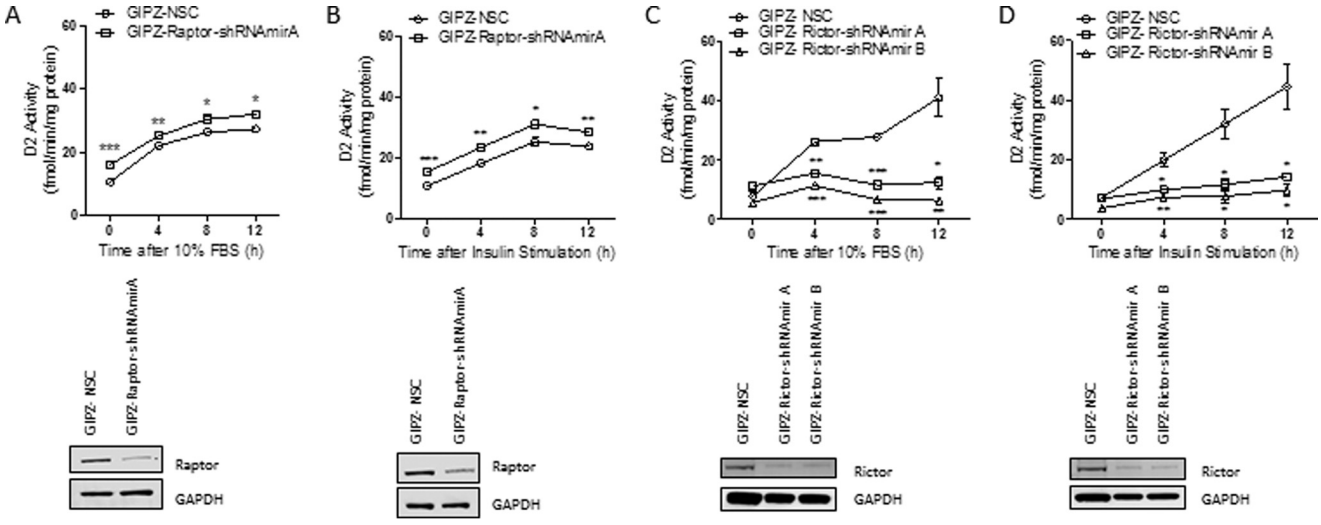

FIGURE 5. **Inhibition of mTORC2 prohibits the insulin-induced increase in D2 activity in MSTO-211H cells.** *A*, *top*, D2 activity measured in MSTO-211H cells stably expressing GIPZ NSC or GIPZ-raptor-shRNAmir A lentiviral vector; cells were serum-starved in 0.1% FBS for 48 h prior to the addition of 10% FBS; $n = 3$; ***, $p < 0.001$ *versus* GIPZ NSC; **, $p < 0.01$ *versus* GIPZ NSC; *, $p < 0.05$ *versus* GIPZ NSC. *Bottom*, Western blot analysis confirming knockdown of rictor using α-total raptor and GAPDH. *B*, *top*, D2 activity measured at various time points in MSTO-211H cells stably expressing GIPZ NSC or GIPZ-raptor-shRNAmir A lentiviral vector; cells were serum-starved in 0.1% FBS for 48 h prior to 600 nM insulin stimulation; $n = 3$; *, $p < 0.05$ *versus* GIPZ NSC; **, $p < 0.01$ *versus* GIPZ NSC; ***, $p < 0.001$ *versus* GIPZ NSC. *Bottom*, Western blot analysis confirming knockdown of rictor using α-total raptor and GAPDH. *C*, *top*, D2 activity measured in MSTO-211H cells stably expressing GIPZ NSC or GIPZ-rictor-shRNAmir A or B lentiviral vectors; cells were serum-starved in 0.1% FBS for 48 h prior to the addition of 10% FBS; $n = 3$; **, $p < 0.01$ *versus* GIPZ NSC; ***, $p < 0.001$ *versus* GIPZ NSC; *, $p < 0.05$ *versus* GIPZ NSC. *Bottom*, Western blot analysis confirming knockdown of rictor using α-total rictor and GAPDH. *D*, *top*, D2 activity measured at various time points in MSTO-211H cells stably expressing GIPZ NSC or GIPZ-rictor-shRNAmir A or B lentiviral vectors; cells were serum-starved in 0.1% FBS for 48 h prior to 600 nM insulin stimulation; $n = 3$; *, $p < 0.05$ *versus* GIPZ NSC; **, $p < 0.01$ *versus* GIPZ NSC. *Bottom*, Western blot analysis confirming knockdown of rictor using α-total rictor and GAPDH. *Error bars*, S.E.

tion of the insulin receptor (LIRKO) and that *Dio2* mRNA levels were restored when this mouse was crossed with a mouse harboring a liver-specific disruption of FOXO1 (LIRFKO) (Fig. 6*A*). This observation, along with previous studies indicating that FOXO3 interacts with the *Dio2* gene (15), suggested that FOXO1 may be the key molecule mediating the effects of nutrient status and insulin signaling on *Dio2*. This suspicion was strengthened by the observation that there was synchronized

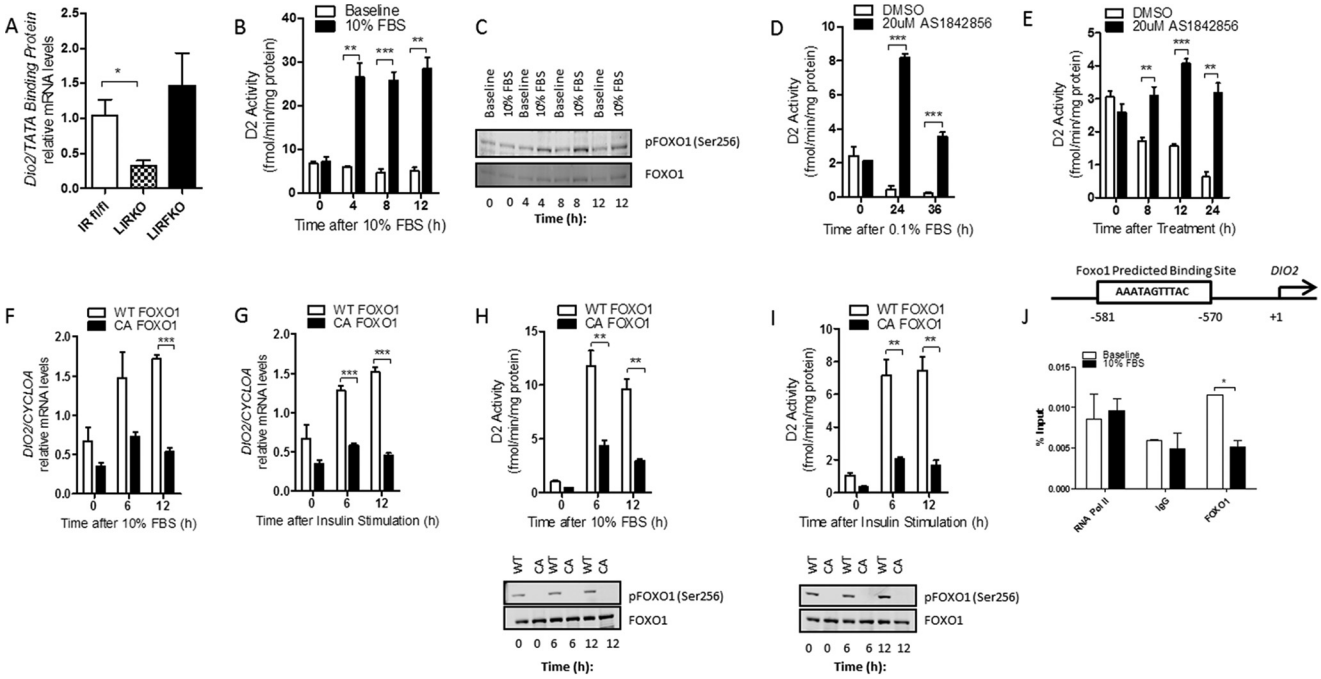

FIGURE 6. **The phosphorylation of FOXO1 or its inhibition using AS1842856 is correlated with an increase in D2 activity, whereas constitutive activation of FOXO1 abrogates the insulin and FBS-induced stimulation in D2 activity in MSTO-211H cells.** *A*, the relative mRNA levels of Dio2/TATA-binding protein in the livers of IR floxed, LIRKO, and LIRFKO mice; $n = 5$, 4, and 6, respectively; *, $p < 0.05$. *B*, D2 activity in cells following 48 h of starvation in 0.1% FBS and the addition of 10% FBS; $n = 3$; **, $p < 0.01$; ***, $p < 0.001$. *C*, corresponding Western blots of phosphorylated and total FOXO1. *D*, D2 activity during starvation in 0.1% FBS with the addition of 20 μM AS1842856; $n = 3$; ***, $p < 0.001$. *E*, D2 activity after 48 h starvation in 0.1% FBS followed by treatment with 20 μM AS1842856; $n = 3$; **, $p < 0.01$; ***, $p < 0.001$. *F*, the measurement of *DIO2/CYCLOA* relative mRNA levels in cells transduced with WT or CA FOXO1 adenoviral vectors following the addition of 10% FBS; $n = 3$; ***, $p < 0.001$. *G*, the measurement of *DIO2/CYCLOA* relative mRNA levels in cells transduced with WT or CA FOXO1 adenoviral vectors following 600 nM insulin stimulation; $n = 3$; ***, $p < 0.001$. *H*, *top*, D2 activity measured in cells transduced with WT or CA FOXO1 adenoviral vectors following the addition of 10% FBS; $n = 3$; **, $p < 0.01$. *Bottom*, corresponding Western blots of phosphorylated and total FOXO1. *I*, *top*, D2 activity measured in cells transduced with WT or CA FOXO1 adenoviral vectors following 600 nM insulin stimulation; $n = 3$; **, $p < 0.01$. *Bottom*, corresponding Western blots of phosphorylated and total FOXO1. *J*, *top*, predicted binding site of FOXO1 on *DIO2* promoter; transcription start site (*TSS*) depicted. *Bottom*, chromatin immunoprecipitation of MSTO-211H cells with anti-FOXO1 antibody followed by RT-qPCR analysis with results presented as percentage of input by control antibody; $n = 2$; *, $p < 0.05$. *Error bars*, S.E.

stimulation of D2 activity and FOXO1 phosphorylation after serum-starved MSTO-211H cells were exposed to 10% FBS (Fig. 6, *B* and *C*). Subsequently, the specific FOXO1 inhibitor AS1842856, which prevents Ser-256 phosphorylation, was added to cells during 0.1% FBS starvation (42). Whereas 0.1% FBS resulted in the expected loss of D2 activity, treatment with AS1842856 not only reversed this but increased D2 activity above baseline levels (Fig. 6*D*). Similar findings were observed in cells that had been starved in 0.1% FBS for 48 h and then treated with AS1842856 (Fig. 6*E*). Taken together, these results indicate that loss of D2 activity associated with fasting is mediated by FOXO1.

To further explore the role of FOXO1 in regulating D2 expression, MSTO-211H cells were infected with WT or CA FOXO1-expressing adenovirus and processed through the 0.1%/10% FBS or insulin stimulation protocols. Remarkably, expression of the CA FOXO1 protein prevents all of the induction of *DIO2* mRNA (Fig. 6, *F* and *G*) and most of the D2 activity (Fig. 6, *H* and *I*) caused by 10% FBS and insulin stimulation. This indicates that *DIO2* is a probable direct target of FOXO1 and that 10% FBS/insulin acts by relieving FOXO1 gene repression. To demonstrate the binding of FOXO1 to predicted binding sites in the *DIO2* promoter region (Fig. 6*J*), ChIP analysis was performed in MSTO-211H cells in 0.1% FBS and 10% FBS. There is specific binding of FOXO1 to a site in the *DIO2* promoter located −570 bp from the transcription start site that is abrogated in refed cells (Fig. 6*J*).

Discussion

The present studies employed a combination of animal and cell models to establish that nutritional availability affects thyroid hormone activation via induction of D2. This enzyme contributes to about two-thirds of the circulating T_3 in humans (about one-third in rodents) and at least one-half of the T_3 present in murine brain and BAT (7). D2 stimulation by 10% FBS is transcriptional and involves insulin and IGF-1 signaling through PI3K-mTORC2-Akt to relieve FOXO1-mediated *DIO2* repression (Fig. 7). These data provide a mechanistic explanation for the observation in humans that fasting is associated with a reduction in skeletal muscle D2 activity that is partially prevented by insulin administration (43). The present findings constitute a new aspect of the overarching homeostatic role played by the hypothalamic-pituitary-thyroid axis to adjust thyroid hormone activation to the appropriate level of energy substrates; thyroidal activity and serum T_3 levels are kept at a minimum (default) during fasting or severe caloric restriction, and both increase as food becomes available.

T_3 receptors (TRs) are ligand-dependent transcription factors that control tissue-specific sets of T_3-responsive genes. TRs are bound to the promoter of T_3-responsive genes, and, as

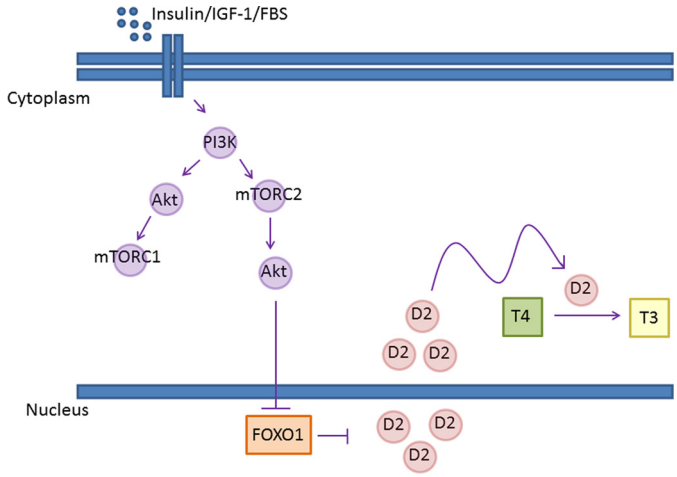

FIGURE 7. **Proposed mechanism of insulin/IGF-1/FBS-mediated stimulation of D2.** Insulin, IGF-1, 10% FBS stimulates D2 transcription and activity via the PI3K-mTORC2-Akt signaling pathway. The inhibitory phosphorylation of FOXO1 by Akt relieves its transcriptional repression on *DIO2*.

opposed to most other receptors, unoccupied TRs actively inhibit transcription, given their affinity for corepressors. Upon binding of T_3, TRs gain affinity for coactivators and trigger T_3-dependent gene transcription. Thus, the role of T_3 is not only to promote expression of T_3-dependent genes but also to relieve TR-mediated gene repression (44). The present observation that fasting shuts down *DIO2* expression (and T_3 production) via shifting the balance between PI3K-mTORC2-Akt and FOXO1 highlights the importance of unoccupied TRs.

D2 expression in the cerebral cortex was not modified by fasting or refeeding (Fig. 1*F*), indicating that *Dio2* regulation by nutrient availability is not universal, probably occurring in tissues where the metabolic pathways are responsive to T_3 and insulin (*e.g.* BAT and skeletal muscle) (7). D2-generated T_3 in BAT enhances local thyroid hormone signaling and the expression of *Ucp1* and *Pgc-1α*, both critical for thermogenesis (45). A local role for D2-generated T_3 in skeletal muscle is less clear. The fact that skeletal muscle physiology is T_3-sensitive (46) sets the stage for a potential D2 contribution, such as during development and response to injury (47). Nevertheless, selective D2 inactivation in the mouse skeletal muscle failed to identify a metabolic phenotype, and serum T_3 was preserved due to increased thyroidal T_3 production (48, 49). The present findings are particularly relevant because the thyroid gland *does not* adjust T_3 production during fasting (8), and serum T_3 drops also as a consequence of FOXO1-mediated *DIO2* inhibition.

In addition, the present findings are clinically relevant because there are ~10 million hypothyroid individuals in the United States alone who depend >80% on the D2 pathway to convert levothyroxine to T_3. Because these patients are hypothyroid, they lack the ability to compensate for FOXO1-mediated *DIO2* suppression during fasting. Thus, serum T_3 levels in these individuals could fluctuate substantially with caloric intake. In many aspects, the balance between PI3K-mTORC2-Akt and FOXO1 signaling should provide nutritional input and fine tuning to the regulation of circulating T_3 levels and T_3-dependent processes.

The data from the LIRKO and LIRFKO mice indicate that insulin is probably a key molecule mediating *Dio2* regulation (Fig. 6*A*), known to provide nutritional input through the PI3K-mTOR signaling pathway in many other systems (50). In the cell model, both insulin and IGF-1 stimulate D2 (Fig. 2, *K* and *L*), indicating that this is an insulin/IGF-1-mediated mechanism. mTOR, which is downstream of insulin/IGF-1 signaling, also plays a central role in defining the balance between anabolic and catabolic processes (51). Downstream targets of mTORC2 include the AGC kinases (*i.e.* Akt, SGK, and PKC*α*, which function to promote cell survival, metabolism, and actin organization) (41). In turn, Akt directly phosphorylates FOXO1 (25, 52), a nuclear transcription factor that modulates multiple sets of genes in a tissue-specific manner (53, 54).

A functional FOXO3 binding site is located in the 5′-UTR of the human *DIO2*, positively regulating *DIO2* expression in developing skeletal muscle (15). Although proteins in the FOXO family can potentially bind to the same DNA cis-elements, the FOXO1 binding site identified in the present studies is within the *DIO2* promoter, close to the transcription start site. Binding of FOXO1 to this site (Fig. 6*J*) suppresses *DIO2* gene expression.

In conclusion, the present study reveals that insulin/IGF-1 transcriptionally up-regulates *DIO2* expression and activity via signaling through the PI3K-mTORC2-Akt pathway, relieving FOXO1-mediated *DIO2* inhibition. D2 is a major contributor to plasma T_3 levels in rodents and in humans and is the predominant pathway producing T_3 in hypothyroid individuals treated with levothyroxine. Therefore, the PI3K-mTORC2-Akt pathway is likely to have major metabolic consequences because it provides a coupling mechanism between nutrient availability and thyroid hormone activation.

Author Contributions—L. J. L. conducted experiments, analyzed and interpreted the data, and prepared the manuscript. J. P. W. and I. O. conducted experiments and analyzed data. T. G. U. created the LIRKO and LIRFKO mice, directed the experiments with these animals, and reviewed/edited the manuscript. A. C. B. directed the studies, interpreted the data, and prepared the manuscript along with L. J. L.

Acknowledgments—We are grateful to John Harney for pointing out that D2 activity in cultured cells increases after a change in the medium; we thank Balázs Gereben for valuable discussions regarding the manuscript; we thank Manish Tandon for assistance with the ChIP experiments.

References

1. Park, H. K., and Ahima, R. S. (2015) Physiology of leptin: energy homeostasis, neuroendocrine function and metabolism. *Metabolism* **64,** 24–34
2. Burger, A. G., Berger, M., Wimpfheimer, K., and Danforth, E. (1980) Interrelationships between energy metabolism and thyroid hormone metabolism during starvation in the rat. *Acta Endocrinol.* **93,** 322–331
3. O'Brian, J. T., Bybee, D. E., Burman, K. D., Osburne, R. C., Ksiazek, M. R., Wartofsky, L., and Georges, L. P. (1980) Thyroid hormone homeostasis in states of relative caloric deprivation. *Metabolism* **29,** 721–727
4. Schebendach, J. E., Golden, N. H., Jacobson, M. S., Hertz, S., and Shenker, I. R. (1997) The metabolic responses to starvation and refeeding in adolescents with anorexia nervosa. *Ann. N.Y. Acad. Sci.* **817,** 110–119
5. Boelen, A., Wiersinga, W. M., and Fliers, E. (2008) Fasting-induced changes in the hypothalamus-pituitary-thyroid axis. *Thyroid* **18,** 123–129
6. Chan, J. L., Heist, K., DePaoli, A. M., Veldhuis, J. D., and Mantzoros, C. S.

(2003) The role of falling leptin levels in the neuroendocrine and metabolic adaptation to short-term starvation in healthy men. *J. Clin. Invest.* **111,** 1409–1421
7. Gereben, B., Zavacki, A. M., Ribich, S., Kim, B. W., Huang, S. A., Simonides, W. S., Zeöld, A., and Bianco, A. C. (2008) Cellular and molecular basis of deiodinase-regulated thyroid hormone signaling. *Endocr. Rev.* **29,** 898–938
8. Kinlaw, W. B., Schwartz, H. L., and Oppenheimer, J. H. (1985) Decreased serum triiodothyronine in starving rats is due primarily to diminished thyroidal secretion of thyroxine. *J. Clin. Invest.* **75,** 1238–1241
9. Vella, K. R., Ramadoss, P., Lam, F. S., Harris, J. C., Ye, F. D., Same, P. D., O'Neill, N. F., Maratos-Flier, E., and Hollenberg, A. N. (2011) NPY and MC4R signaling regulate thyroid hormone levels during fasting through both central and peripheral pathways. *Cell Metab.* **14,** 780–790
10. Galton, V. A., Hernandez, A., and St Germain, D. L. (2014) The 5′-deiodinases are not essential for the fasting-induced decrease in circulating thyroid hormone levels in male mice: possible roles for the type 3 deiodinase and tissue sequestration of hormone. *Endocrinology* **155,** 3172–3181
11. Balsam, A., and Ingbar, S. H. (1978) The influence of fasting, diabetes, and several pharmacological agents on the pathways of thyroxine metabolism in rat liver. *J. Clin. Invest.* **62,** 415–424
12. Zavacki, A. M., Ying, H., Christoffolete, M. A., Aerts, G., So, E., Harney, J. W., Cheng, S. Y., Larsen, P. R., and Bianco, A. C. (2005) Type 1 iodothyronine deiodinase is a sensitive marker of peripheral thyroid status in the mouse. *Endocrinology* **146,** 1568–1575
13. Bianco, A. C. (2011) Minireview: cracking the metabolic code for thyroid hormone signaling. *Endocrinology* **152,** 3306–3311
14. Gereben, B., and Salvatore, D. (2005) Pretranslational regulation of type 2 deiodinase. *Thyroid* **15,** 855–864
15. Dentice, M., Marsili, A., Ambrosio, R., Guardiola, O., Sibilio, A., Paik, J. H., Minchiotti, G., DePinho, R. A., Fenzi, G., Larsen, P. R., and Salvatore, D. (2010) The FoxO3/type 2 deiodinase pathway is required for normal mouse myogenesis and muscle regeneration. *J. Clin. Invest.* **120,** 4021–4030
16. Arrojo E Drigo, R., Fonseca, T. L., Castillo, M., Salathe, M., Simovic, G., Mohácsik, P., Gereben, B., and Bianco, A. C. (2011) Endoplasmic reticulum stress decreases intracellular thyroid hormone activation via an eIF2a-mediated decrease in type 2 deiodinase synthesis. *Mol. Endocrinol.* **25,** 2065–2075
17. Sagar, G. D., Gereben, B., Callebaut, I., Mornon, J. P., Zeöld, A., da Silva, W. S., Luongo, C., Dentice, M., Tente, S. M., Freitas, B. C., Harney, J. W., Zavacki, A. M., and Bianco, A. C. (2007) Ubiquitination-induced conformational change within the deiodinase dimer is a switch regulating enzyme activity. *Mol. Cell. Biol.* **27,** 4774–4783
18. Martinez-deMena, R., and Obregón, M. J. (2005) Insulin increases the adrenergic stimulation of 5′ deiodinase activity and mRNA expression in rat brown adipocytes; role of MAPK and PI3K. *J. Mol. Endocrinol.* **34,** 139–151
19. Mills, I., Barge, R. M., Silva, J. E., and Larsen, P. R. (1987) Insulin stimulation of iodothyronine 5′-deiodinase in rat brown adipocytes. *Biochem. Biophys. Res. Commun.* **143,** 81–86
20. Laplante, M., and Sabatini, D. M. (2009) mTOR signaling at a glance. *J. Cell Sci.* **122,** 3589–3594
21. Hoeffer, C. A., and Klann, E. (2010) mTOR signaling: at the crossroads of plasticity, memory and disease. *Trends Neurosci.* **33,** 67–75
22. Frost, R. A., and Lang, C. H. (2011) mTor signaling in skeletal muscle during sepsis and inflammation: where does it all go wrong? *Physiology* **26,** 83–96
23. Thoreen, C. C., Chantranupong, L., Keys, H. R., Wang, T., Gray, N. S., and Sabatini, D. M. (2012) A unifying model for mTORC1-mediated regulation of mRNA translation. *Nature* **485,** 109–113
24. Düvel, K., Yecies, J. L., Menon, S., Raman, P., Lipovsky, A. I., Souza, A. L., Triantafellow, E., Ma, Q., Gorski, R., Cleaver, S., Vander Heiden, M. G., MacKeigan, J. P., Finan, P. M., Clish, C. B., Murphy, L. O., and Manning, B. D. (2010) Activation of a metabolic gene regulatory network downstream of mTOR complex 1. *Mol. Cell* **39,** 171–183
25. Su, B., and Jacinto, E. (2011) Mammalian TOR signaling to the AGC kinases. *Crit. Rev. Biochem. Mol. Biol.* **46,** 527–547
26. Ma, X. M., and Blenis, J. (2009) Molecular mechanisms of mTOR-mediated translational control. *Nat. Rev. Mol. Cell Biol.* **10,** 307–318
27. Grozovsky, R., Ribich, S., Rosene, M. L., Mulcahey, M. A., Huang, S. A., Patti, M. E., Bianco, A. C., and Kim, B. W. (2009) Type 2 deiodinase expression is induced by peroxisomal proliferator-activated receptor-γ agonists in skeletal myocytes. *Endocrinology* **150,** 1976–1983
28. Mills, I., Raasmaja, A., Moolten, N., Lemack, G., Silva, J. E., and Larsen, P. R. (1989) Effect of thyroid status on catecholamine stimulation of thyroxine 5′-deiodinase in brown adipocytes. *Am. J. Physiol.* **256,** E74–E79
29. Bianco, A. C., Anderson, G., Forrest, D., Galton, V. A., Gereben, B., Kim, B. W., Kopp, P. A., Liao, X. H., Obregon, M. J., Peeters, R. P., Refetoff, S., Sharlin, D. S., Simonides, W. S., Weiss, R. E., Williams, G. R., American Thyroid Association Task Force on Approaches and Strategies to Investigate Thyroid Hormone Economy and Action (2014) American thyroid association guide to investigating thyroid hormone economy and action in rodent and cell models. *Thyroid* **24,** 88–168
30. Curcio, C., Baqui, M. M., Salvatore, D., Rihn, B. H., Mohr, S., Harney, J. W., Larsen, P. R., and Bianco, A. C. (2001) The human type 2 iodothyronine deiodinase is a selenoprotein highly expressed in a mesothelioma cell line. *J. Biol. Chem.* **276,** 30183–30187
31. da-Silva, W. S., Harney, J. W., Kim, B. W., Li, J., Bianco, S. D., Crescenzi, A., Christoffolete, M. A., Huang, S. A., and Bianco, A. C. (2007) The small polyphenolic molecule kaempferol increases cellular energy expenditure and thyroid hormone activation. *Diabetes* **56,** 767–776
32. Zhang, W., Patil, S., Chauhan, B., Guo, S., Powell, D. R., Le, J., Klotsas, A., Matika, R., Xiao, X., Franks, R., Heidenreich, K. A., Sajan, M. P., Farese, R. V., Stolz, D. B., Tso, P., Koo, S. H., Montminy, M., and Unterman, T. G. (2006) FoxO1 regulates multiple metabolic pathways in the liver: effects on gluconeogenic, glycolytic, and lipogenic gene expression. *J. Biol. Chem.* **281,** 10105–10117
33. O-Sullivan, I., Zhang, W., Wasserman, D. H., Liew, C. W., Liu, J., Paik, J., DePinho, R. A., Stolz, D. B., Kahn, C. R., Schwartz, M. W., and Unterman, T. G. (2015) FoxO1 integrates direct and indirect effects of insulin on hepatic glucose production and glucose utilization. *Nat. Commun.* **6,** 7079
34. Ferrara, A. M., Liao, X. H., Gil-Ibáñez, P., Marcinkowski, T., Bernal, J., Weiss, R. E., Dumitrescu, A. M., and Refetoff, S. (2013) Changes in thyroid status during perinatal development of MCT8-deficient male mice. *Endocrinology* **154,** 2533–2541
35. Arrojo E Drigo, R., and Bianco, A. C. (2011) Type 2 deiodinase at the crossroads of thyroid hormone action. *Int. J. Biochem. Cell Biol.* **43,** 1432–1441
36. Levy, D. S., Kahana, J. A., and Kumar, R. (2009) AKT inhibitor, GSK690693, induces growth inhibition and apoptosis in acute lymphoblastic leukemia cell lines. *Blood* **113,** 1723–1729
37. Carol, H., Morton, C. L., Gorlick, R., Kolb, E. A., Keir, S. T., Reynolds, C. P., Kang, M. H., Maris, J. M., Billups, C., Smith, M. A., Houghton, P. J., and Lock, R. B. (2010) Initial testing (stage 1) of the Akt inhibitor GSK690693 by the pediatric preclinical testing program. *Pediatr. Blood Cancer* **55,** 1329–1337
38. Feldman, M. E., Apsel, B., Uotila, A., Loewith, R., Knight, Z. A., Ruggero, D., and Shokat, K. M. (2009) Active-site inhibitors of mTOR target rapamycin-resistant outputs of mTORC1 and mTORC2. *PLoS Biol.* **7,** e38
39. Guertin, D. A., and Sabatini, D. M. (2009) The pharmacology of mTOR inhibition. *Sci. Signal.* **2,** pe24
40. Dowling, R. J., Topisirovic, I., Fonseca, B. D., and Sonenberg, N. (2010) Dissecting the role of mTOR: lessons from mTOR inhibitors. *Biochim. Biophys. Acta* **1804,** 433–439
41. Oh, W. J., and Jacinto, E. (2011) mTOR complex 2 signaling and functions. *Cell Cycle* **10,** 2305–2316
42. Nagashima, T., Shigematsu, N., Maruki, R., Urano, Y., Tanaka, H., Shimaya, A., Shimokawa, T., and Shibasaki, M. (2010) Discovery of novel forkhead box O1 inhibitors for treating type 2 diabetes: improvement of fasting glycemia in diabetic db/db mice. *Mol. Pharmacol.* **78,** 961–970
43. Heemstra, K. A., Soeters, M. R., Fliers, E., Serlie, M. J., Burggraaf, J., van Doorn, M. B., van der Klaauw, A. A., Romijn, J. A., Smit, J. W., Corssmit, E. P., and Visser, T. J. (2009) Type 2 iodothyronine deiodinase in skeletal muscle: effects of hypothyroidism and fasting. *J. Clin. Endocrinol. Metab.* **94,** 2144–2150

44. Brent, G. A. (2012) Mechanisms of thyroid hormone action. *J. Clin. Invest.* **122,** 3035–3043
45. Hall, J. A., Ribich, S., Christoffolete, M. A., Simovic, G., Correa-Medina, M., Patti, M. E., and Bianco, A. C. (2010) Absence of thyroid hormone activation during development underlies a permanent defect in adaptive thermogenesis. *Endocrinology* **151,** 4573–4582
46. Simonides, W. S., and van Hardeveld, C. (2008) Thyroid hormone as a determinant of metabolic and contractile phenotype of skeletal muscle. *Thyroid* **18,** 205–216
47. Dentice, M., Ambrosio, R., Damiano, V., Sibilio, A., Luongo, C., Guardiola, O., Yennek, S., Zordan, P., Minchiotti, G., Colao, A., Marsili, A., Brunelli, S., Del Vecchio, L., Larsen, P. R., Tajbakhsh, S., and Salvatore, D. (2014) Intracellular inactivation of thyroid hormone is a survival mechanism for muscle stem cell proliferation and lineage progression. *Cell Metab.* **20,** 1038–1048
48. Fonseca, T. L., Werneck-De-Castro, J. P., Castillo, M., Bocco, B. M., Fernandes, G. W., McAninch, E. A., Ignacio, D. L., Moises, C. C., Ferreira, A. R., Gereben, B., and Bianco, A. C. (2014) Tissue-specific inactivation of type 2 deiodinase reveals multilevel control of fatty acid oxidation by thyroid hormone in the mouse. *Diabetes* **63,** 1594–1604
49. Werneck-de-Castro, J. P., Fonseca, T. L., Ignacio, D. L., Fernandes, G. W., Andrade-Feraud, C. M., Lartey, L. J., Ribeiro, M. B., Ribeiro, M. O., Gereben, B., and Bianco, A. C. (2015) Thyroid hormone signaling in male mouse skeletal muscle is largely independent of D2 in myocytes. *Endocrinology* **156,** 3842–3852
50. Hay, N., and Sonenberg, N. (2004) Upstream and downstream of mTOR. *Genes Dev.* **18,** 1926–1945
51. Kim, S. G., Buel, G. R., and Blenis, J. (2013) Nutrient regulation of the mTOR complex 1 signaling pathway. *Mol. Cells* **35,** 463–473
52. Nakae, J., Kitamura, T., Kitamura, Y., Biggs, W. H., 3rd, Arden, K. C., and Accili, D. (2003) The forkhead transcription factor Foxo1 regulates adipocyte differentiation. *Dev. Cell* **4,** 119–129
53. Barthel, A., Schmoll, D., and Unterman, T. G. (2005) FoxO proteins in insulin action and metabolism. *Trends Endocrinol. Metab.* **16,** 183–189
54. Matsumoto, M., Han, S., Kitamura, T., and Accili, D. (2006) Dual role of transcription factor FoxO1 in controlling hepatic insulin sensitivity and lipid metabolism. *J. Clin. Invest.* **116,** 2464–2472